

## **INVESTIGATION OF LOCALLY LOADED MULTILAYER SHELLS BY A MIXED FINITE-ELEMENT METHOD.**

### **1. GEOMETRICALLY LINEAR STATEMENT**

**G. M. Kulikov and S. V. Plotnikova**

*Keywords: multilayer shell, finite-element method, mixed model, rubber-cord composite*

*The Hu–Washizu functional is constructed for analyzing prestressed multilayer anisotropic Timoshenko-type shells. As unknown functions, six displacements and eleven strains of the faces of the shells are chosen. Based on mixed finite-element approximations, a numerical algorithm is developed for solving linear static problems of prestressed multilayer composite shells. The results of solving the well-known test problem on a cylindrical shell subjected to two opposite point forces and the problem on local loading of a toroidal multilayer rubber-cord shell are presented.*

### **Introduction**

The calculation of locally loaded multilayer Timoshenko-type shells without account for transverse compression is presented in [1-4]. The history of the problem and its solution methods, as applied to rubber-cord shells, were adequately analyzed in the reviews [5, 6]. In our study, based on the theory of multilayer anisotropic Timoshenko-type shells and with regard for transverse compression [7], an algorithm for numerical solution of the problem of local loading of multilayer shells is elaborated with the use of mixed finite-element approximations. An important feature of the approach described in [7] is that six displacements of the faces of the shells are chosen as unknown functions. This makes it possible to simplify the statement of contact problems of the mechanics of thin-walled structures [8] and to develop efficient finite elements for Timoshenko-type shells from the viewpoint of precise representation of displacements of a shell element as a rigid unit [9, 10]. This property of the element is very useful in solving problems with a high degree of localization of a load [11, 12].

### **Statement of the Problem**

Let us consider a prestressed thin shell of thickness  $h$  composed of  $N$  elastic anisotropic layers with a constant thickness  $h_k$ . We assume that, at each point of the shell, there is a surface of elastic symmetry parallel to a reference surface. As the reference surface  $S$ , we take either the inner surface of some  $k$ th layer or a contact surface between the layers, which is referred to the curved orthogonal coordinates  $\alpha_1$  and  $\alpha_2$  along the lines of main curvatures. The transverse coordinate  $\alpha_3$  is reckoned in the direction of the increasing external normal to the surface  $S$  (Fig. 1).

---

Tambov State Technical University, Russia. Translated from *Mekhanika Kompozitnykh Materialov*, Vol. 38, No. 5, pp. 607-620, September-October, 2002. Original article submitted January 28, 2002; revision submitted April 22, 2002.

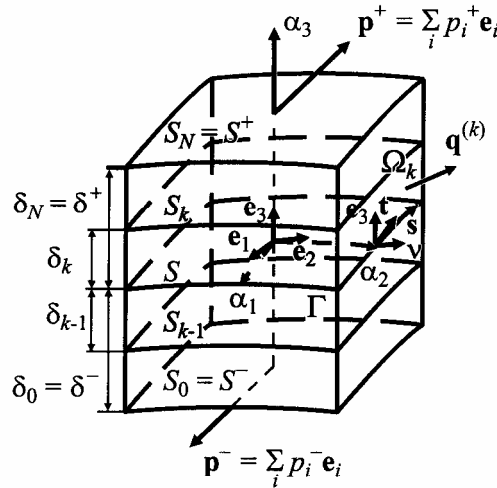


Fig. 1. Scheme of a multilayer shell.

Let  $A_\alpha$  be the Lamé parameters,  $k_\alpha$  the curvatures of the coordinate lines,  $\delta_k$  the distance from the surface  $S$  to the upper boundary surface of a  $k$ th layer  $S_k$ ,  $u_i$  the displacements of points of the shell,  $\varepsilon_{ij}$  the strain-tensor components,  $\sigma_{ij}^{(k)}$  the stress-tensor components of the  $k$ th layer,  $\tau_{ij}^{(k)}$  the components of the tensor of initial stresses of the  $k$ th layer,  $b_{ijlm}^{(k)}$  the stiffness of the  $k$ th layer,  $p_i^-$  and  $p_i^+$  the external surface loads operating on the internal  $S^-$  and external  $S^+$  faces of the shell,  $\mathbf{q}^{(k)} = q_v^{(k)} \mathbf{v} + q_t^{(k)} \mathbf{t} + q_3^{(k)} \mathbf{e}_3$  the vector of external surface loads operating on the lateral surface of the  $k$ th layer  $\Omega_k$ , and  $\mathbf{v}$  and  $\mathbf{t}$  the normal and tangential unit vectors to the boundary contour  $\Gamma$ . Hereinafter,  $k = \overline{1, N}$ ;  $i, j, l, m = 1, 2, 3$ ;  $\alpha, \beta, \gamma, \delta = 1, 2$ .

When formulating the theory of multilayer anisotropic shells, we use the Timoshenko kinematic hypothesis of a linear distribution of tangential displacements across the thickness of the shell [7, 13]

$$u_i = N^-(\alpha_3) v_i^- + N^+(\alpha_3) v_i^+, \quad (1)$$

where  $v_i^\pm(\alpha_1, \alpha_2)$  are the displacements of the faces  $S^\pm$  of the shell and  $N^\pm(\alpha_3)$  are linear functions of the shell shape:

$$N^-(\alpha_3) = \frac{\delta^+ - \alpha_3}{h}, \quad N^+(\alpha_3) = \frac{\alpha_3 - \delta^-}{h}.$$

For the strains, we assume an independent approximation:

$$\begin{aligned} \varepsilon_{\alpha\alpha} &= N^-(\alpha_3) E_{\alpha\alpha}^- + N^+(\alpha_3) E_{\alpha\alpha}^+, \quad \varepsilon_{33} = E_{33}, \\ 2\varepsilon_{ij} &= N^-(\alpha_3) E_{ij}^- + N^+(\alpha_3) E_{ij}^+ \quad (i \neq j), \end{aligned} \quad (2)$$

where  $E_{\alpha\beta}^\pm(\alpha_1, \alpha_2)$  and  $E_{\alpha 3}^\pm(\alpha_1, \alpha_2)$  are the tangential and transverse tangential strains of the faces  $S^\pm$  and  $E_{33}(\alpha_1, \alpha_2)$  is the transverse compression of the shell.

### The Hu–Washizu Functional

As is known, the equilibrium equations, deformation relations, equations of the generalized Hooke's law, and the boundary conditions on the faces and ends of a shell are represented by the Euler equations and natural boundary conditions of a

certain variation problem. In this connection, we introduce independent approximations of displacements (1) and strains (2) into the Hu–Washizu functional of three-dimensional elasticity theory [14] and, using the assumption of thin-wallness of the shell, we come to a formula for the variation of the Hu–Washizu functional for a prestressed multilayer anisotropic shell:

$$\begin{aligned}
 \delta J = & - \iint_S \left\{ \sum_{\alpha \leq i} \left[ H_{\alpha i}^- - \sum_{\beta \leq j} (D_{\alpha i \beta j}^{00} E_{\beta j}^- + D_{\alpha i \beta j}^{01} E_{\beta j}^+) - \underline{D}_{\alpha i 33}^- E_{33} \right] \delta E_{\alpha i}^- \right. \\
 & + \sum_{\alpha \leq i} \left[ H_{\alpha i}^+ - \sum_{\beta \leq j} (D_{\alpha i \beta j}^{01} E_{\beta j}^- + D_{\alpha i \beta j}^{11} E_{\beta j}^+) - \underline{D}_{\alpha i 33}^+ E_{33} \right] \delta E_{\alpha i}^+ \\
 & + \left[ H_{33} - \sum_{\beta \leq j} (D_{33 \beta j}^- E_{\beta j}^- + D_{33 \beta j}^+ E_{\beta j}^+) - D_{3333} E_{33} \right] \delta E_{33} \\
 & + \sum_{\alpha \leq i} [(E_{\alpha i}^- - e_{\alpha i}^-) \delta H_{\alpha i}^- + (E_{\alpha i}^+ - e_{\alpha i}^+) \delta H_{\alpha i}^+ - H_{\alpha i}^- \delta e_{\alpha i}^- - H_{\alpha i}^+ \delta e_{\alpha i}^+ \\
 & - L_{\alpha i}^- \delta \eta_{\alpha i}^- - L_{\alpha i}^+ \delta \eta_{\alpha i}^+] + (E_{33} - e_{33}) \delta H_{33} - H_{33} \delta e_{33} - L_{33} \delta \eta_{33} \\
 & \left. + \sum_i (p_i^+ \delta v_i^+ - p_i^- \delta v_i^-) \right\} A_1 A_2 d\alpha_1 d\alpha_2 \\
 & - \oint_{\Gamma} (\hat{H}_{\nu\nu}^- \delta v_{\nu}^- + \hat{H}_{\nu\nu}^+ \delta v_{\nu}^+ + \hat{H}_{\nu i}^- \delta v_i^- + \hat{H}_{\nu i}^+ \delta v_i^+ + \hat{H}_{\nu 3}^- \delta v_3^- + \hat{H}_{\nu 3}^+ \delta v_3^+) ds, \tag{3}
 \end{aligned}$$

where

$$\begin{aligned}
 e_{\gamma\gamma}^{\pm} &= \frac{1}{\zeta_{\gamma}^{\pm}} \lambda_{\gamma}^{\pm}, \quad e_{12}^{\pm} = \frac{1}{\zeta_1^{\pm}} \omega_1^{\pm} + \frac{1}{\zeta_2^{\pm}} \omega_2^{\pm}, \quad e_{\gamma 3}^{\pm} = \left( 1 \pm \frac{k_{\gamma} h}{2 \bar{\zeta}_{\gamma}} \right) \beta_{\gamma} - \frac{1}{\bar{\zeta}_{\gamma}} \theta_{\gamma}^{\pm}, \\
 e_{33} = \beta_3, \eta_{\gamma\gamma}^{\pm} &= \frac{1}{2(\zeta_{\gamma}^{\pm})^2} [(\lambda_{\gamma}^{\pm})^2 + (\omega_{\gamma}^{\pm})^2 + (\theta_{\gamma}^{\pm})^2], \eta_{12}^{\pm} = \frac{1}{\zeta_1^{\pm} \zeta_2^{\pm}} (\lambda_1^{\pm} \omega_2^{\pm} + \lambda_2^{\pm} \omega_1^{\pm} + \theta_1^{\pm} \theta_2^{\pm}), \\
 \eta_{\gamma 3}^{\pm} &= \frac{1}{\bar{\zeta}_{\gamma}} (\beta_{\gamma} \lambda_{\gamma}^{\pm} + \beta_{\delta} \omega_{\gamma}^{\pm} - \beta_3 \theta_{\gamma}^{\pm}), \quad \eta_{33} = \frac{1}{2} (\beta_1^2 + \beta_2^2 + \beta_3^2), \tag{4} \\
 \lambda_{\gamma}^{\pm} &= \frac{1}{A_{\gamma}} \frac{\partial v_{\gamma}^{\pm}}{\partial \alpha_{\gamma}} + B_{\delta} v_{\delta}^{\pm} + k_{\gamma} v_3^{\pm}, \quad \omega_{\gamma}^{\pm} = \frac{1}{A_{\gamma}} \frac{\partial v_{\delta}^{\pm}}{\partial \alpha_{\gamma}} - B_{\delta} v_{\gamma}^{\pm}, \\
 \theta_{\gamma}^{\pm} &= -\frac{1}{A_{\gamma}} \frac{\partial v_3^{\pm}}{\partial \alpha_{\gamma}} + k_{\gamma} v_{\gamma}^{\pm}, \quad \beta_i = \frac{1}{h} (v_i^+ - v_i^-), \quad B_{\gamma} = \frac{1}{A_1 A_2} \frac{\partial A_{\delta}}{\partial \alpha_{\gamma}} \quad (\delta \neq \gamma), \\
 \zeta_{\gamma}^{\pm} &= 1 + k_{\gamma} \delta^{\pm}, \quad \bar{\zeta}_{\gamma} = 1 + k_{\gamma} \bar{\delta}, \quad \bar{\delta} = \frac{1}{2} (\delta^- + \delta^+)
 \end{aligned}$$

Here,  $v_v^\pm$ ,  $v_t^\pm$ , and  $v_3^\pm$  are the components of displacements of the faces  $S^\pm$  in the local basis  $\mathbf{v}$ ,  $\mathbf{t}$ , and  $\mathbf{e}_3$  (see Fig. 1),  $H_{\alpha i}^\pm$  and  $H_{33}$  are the resultants of stresses,  $L_{\alpha i}^\pm$  and  $L_{33}$  are the resultants of initial stresses, and  $\hat{H}_{v v}^\pm$ ,  $\hat{H}_{v t}^\pm$ , and  $\hat{H}_{v 3}^\pm$  are the resultants of external surface loads, which can be found from the formulas

$$D_{ijlm}^{pq} = \sum_{k=1}^N \int_{\delta_{k-1}}^{\delta_k} b_{ijlm}^{(k)} [N^-(\alpha_3)]^{2-p-q} [N^+(\alpha_3)]^{p+q} d\alpha_3 \quad (p, q = 0, 1), \quad (5)$$

$$D_{ij33}^- = D_{ij33}^{00} + D_{ij33}^{01}, \quad D_{ij33}^+ = D_{ij33}^{01} + D_{ij33}^{11}, \quad D_{3333} = D_{3333}^- + D_{3333}^+,$$

$$H_{\alpha i}^\pm = \sum_{k=1}^N \int_{\delta_{k-1}}^{\delta_k} \sigma_{\alpha i}^{(k)} N^\pm(\alpha_3) d\alpha_3, \quad H_{33} = \sum_{k=1}^N \int_{\delta_{k-1}}^{\delta_k} \sigma_{33}^{(k)} d\alpha_3,$$

$$L_{\alpha i}^\pm = \sum_{k=1}^N \int_{\delta_{k-1}}^{\delta_k} \tau_{\alpha i}^{(k)} N^\pm(\alpha_3) d\alpha_3, \quad L_{33} = \sum_{k=1}^N \int_{\delta_{k-1}}^{\delta_k} \tau_{33}^{(k)} d\alpha_3, \quad (6)$$

$$\hat{H}_{vs}^\pm = \sum_{k=1}^N \int_{\delta_{k-1}}^{\delta_k} q_s^{(k)} N^\pm(\alpha_3) d\alpha_3 \quad (s = v, t, 3).$$

In Eq. (5),  $b_{\alpha\beta\gamma 3}^{(k)} = b_{\alpha 333}^{(k)} = 0$ .

The stress tensor can be calculated from the generalized Hooke's law

$$\sigma_{ij}^{(k)} = \sum_{l,m} b_{ijlm}^{(k)} \varepsilon_{lm}. \quad (7)$$

However, for calculating shells of incompressible or nearly incompressible materials, in particular, rubber-cord ones, for which the Poisson ratios are close to 0.5, elasticity relations (7) are of little use. This inconsistency can be overcome by using the assumption of thin-wallness of the shell and accordingly taking that  $b_{\alpha\beta 33}^{(k)} = 0$  [7]. At the same time, for the normal stress  $\sigma_{33}^{(k)}$ , Eq. (7) is left unchanged. The aforesaid means that the underlined terms in formula (3) must be omitted. As a result, we come to an asymmetric stiffness matrix of the shell [7], which however does not bring about considerable corrections in the numerical realization of the problem by the mixed finite-element model.

We should also note that the Hu–Washizu functional (3)-(6) generalizes the corresponding functional for geometrically linear multilayer shells [9] to the case where the prestressed state is taken into account.

### Numerical Solution Algorithm for Linear Static Problems of Multilayer Anisotropic Shells

Let us consider the problem of local loading of a prestressed anisotropic multilayer shell in a geometrically linear statement (a more general statement will be discussed in the second report). It can be proved [9] that, in this case, deformation relations (4), which serve as a basis for the Hu–Washizu functional, precisely represent displacements of the shell as a rigid body. This property of deformation relations (4) is crucial in calculating shells with a high degree of localization of a load, including those subjected to concentrated actions.

Taking into account the adopted assumptions, the variation of the Hu–Washizu functional, Eq. (3), for a shell element in its local coordinates  $\xi_1$  and  $\xi_2$  can be presented in the matrix form

$$\delta J^{el} = - \int_{-1}^1 \int_{-1}^1 [(\mathbf{H} - \mathbf{D}\mathbf{E})^T \delta \mathbf{E} + (\mathbf{E} - \mathbf{e})^T \delta \mathbf{H} - \mathbf{H}^T \delta \mathbf{e} - \mathbf{L}^T \delta \boldsymbol{\eta} + \mathbf{P}^T \delta \mathbf{v}] \Lambda d\xi_1 d\xi_2 - \oint_{\Gamma^{el}} \hat{\mathbf{H}}_{\Gamma}^T \delta \mathbf{v}_{\Gamma} ds,$$

$$\mathbf{v} = [v_1^- \ v_1^+ \ v_2^- \ v_2^+ \ v_3^- \ v_3^+]^T, \quad \mathbf{v}_{\Gamma} = [v_v^- \ v_v^+ \ v_t^- \ v_t^+ \ v_3^- \ v_3^+]^T,$$

$$\mathbf{P} = [-p_1^- \ p_1^+ \ -p_2^- \ p_2^+ \ -p_3^- \ p_3^+]^T, \quad \hat{\mathbf{H}}_{\Gamma} = [\hat{H}_{vv}^- \ \hat{H}_{vv}^+ \ \hat{H}_{vt}^- \ \hat{H}_{vt}^+ \ \hat{H}_{v3}^- \ \hat{H}_{v3}^+]^T,$$

$$\mathbf{e} = [e_{11}^- \ e_{11}^+ \ e_{22}^- \ e_{22}^+ \ e_{12}^- \ e_{12}^+ \ e_{13}^- \ e_{13}^+ \ e_{23}^- \ e_{23}^+ \ e_{33}^- \ e_{33}^+]^T, \quad \boldsymbol{\eta} = [\eta_{11}^- \ \eta_{11}^+ \ \eta_{22}^- \ \eta_{22}^+ \ \eta_{12}^- \ \eta_{12}^+ \ \eta_{13}^- \ \eta_{13}^+ \ \eta_{23}^- \ \eta_{23}^+ \ \eta_{33}^- \ \eta_{33}^+]^T,$$

$$\mathbf{E} = [E_{11}^- \ E_{11}^+ \ E_{22}^- \ E_{22}^+ \ E_{12}^- \ E_{12}^+ \ E_{13}^- \ E_{13}^+ \ E_{23}^- \ E_{23}^+ \ E_{33}^- \ E_{33}^+]^T, \quad (8)$$

$$\mathbf{H} = [H_{11}^- \ H_{11}^+ \ H_{22}^- \ H_{22}^+ \ H_{12}^- \ H_{12}^+ \ H_{13}^- \ H_{13}^+ \ H_{23}^- \ H_{23}^+ \ H_{33}^- \ H_{33}^+]^T,$$

$$\mathbf{L} = [L_{11}^- \ L_{11}^+ \ L_{22}^- \ L_{22}^+ \ L_{12}^- \ L_{12}^+ \ L_{13}^- \ L_{13}^+ \ L_{23}^- \ L_{23}^+ \ L_{33}^- \ L_{33}^+]^T,$$

where  $\Lambda(\xi_1, \xi_2)$  is a function characterizing the metrics of the element,  $\mathbf{v}$  is the displacement vector,  $\mathbf{v}_{\Gamma}$  is the displacement vector of the boundary contour of the element  $\Gamma^{el}$ ,  $\mathbf{E}$ ,  $\mathbf{e}$ , and  $\boldsymbol{\eta}$  are vectors characterizing the deformation relations,  $\mathbf{H}$  is the vector of resulting stresses,  $\mathbf{L}$  is the vector of resulting initial stresses,  $\hat{\mathbf{H}}_{\Gamma}$  is the vector of resulting loads operating on the boundary of the element  $\Gamma^{el}$ ,  $\mathbf{P}$  is the vector of surface loads, and  $\mathbf{D}$  is an asymmetric  $11 \times 11$  matrix of elastic coefficients, whose elements are determined from relations (5) and those given in [7] for incompressible resin-like materials.

In functional (8), the vectors  $\mathbf{v}$ ,  $\mathbf{E}$ , and  $\mathbf{H}$  are independent functional variables, therefore, independent approximations must be used for them on the element considered. For displacements, we employ the standard bilinear approximation

$$\mathbf{v} = \sum_r N_r \mathbf{v}_r, \quad (9)$$

where  $N_r(\xi_1, \xi_2)$  are linear shape functions and  $\mathbf{v}_r = [v_{1r}^- \ v_{1r}^+ \ v_{2r}^- \ v_{2r}^+ \ v_{3r}^- \ v_{3r}^+]^T$  are the vectors of nodal displacements ( $r = \overline{1, 4}$ ).

For the strains, according to the method of double approximation [15, 16], generalized to the case of transverse compression, we have even simpler formulas:

$$\mathbf{E} = \sum_{\eta_1, \eta_2} \mathbf{Q}^{\eta_1 \eta_2} \mathbf{E}^{\eta_1 \eta_2} \xi_1^{\eta_1} \xi_2^{\eta_2}, \quad (10)$$

$$\mathbf{E}^{00} = [E_{11}^{-00} \ E_{11}^{+00} \ E_{22}^{-00} \ E_{22}^{+00} \ E_{12}^{-00} \ E_{12}^{+00} \ E_{13}^{-00} \ E_{13}^{+00} \ E_{23}^{-00} \ E_{23}^{+00} \ E_{33}^{00}]^T,$$

$$\mathbf{E}^{01} = [E_{11}^{-01} \ E_{11}^{+01} \ E_{13}^{-01} \ E_{13}^{+01} \ E_{33}^{01}]^T, \quad \mathbf{E}^{10} = [E_{22}^{-10} \ E_{22}^{+10} \ E_{23}^{-10} \ E_{23}^{+10} \ E_{33}^{10}]^T,$$

$$\mathbf{E}^{11} = [E_{33}^{11}], \quad (11)$$

$$\mathbf{Q}^{01} = \begin{bmatrix} 1 & 0 & 0 & 0 & 0 \\ 0 & 1 & 0 & 0 & 0 \\ 0 & 0 & 0 & 0 & 0 \\ 0 & 0 & 0 & 0 & 0 \\ 0 & 0 & 0 & 0 & 0 \\ 0 & 0 & 0 & 0 & 0 \\ 0 & 0 & 1 & 0 & 0 \\ 0 & 0 & 0 & 1 & 0 \\ 0 & 0 & 0 & 0 & 0 \\ 0 & 0 & 0 & 0 & 0 \\ 0 & 0 & 0 & 0 & 1 \end{bmatrix}, \quad \mathbf{Q}^{10} = \begin{bmatrix} 0 & 0 & 0 & 0 & 0 \\ 0 & 0 & 0 & 0 & 0 \\ 1 & 0 & 0 & 0 & 0 \\ 0 & 1 & 0 & 0 & 0 \\ 0 & 0 & 0 & 0 & 0 \\ 0 & 0 & 0 & 0 & 0 \\ 0 & 0 & 0 & 0 & 0 \\ 0 & 0 & 0 & 0 & 0 \\ 0 & 0 & 1 & 0 & 0 \\ 0 & 0 & 0 & 1 & 0 \\ 0 & 0 & 0 & 0 & 1 \end{bmatrix}, \quad \mathbf{Q}^{11} = \begin{bmatrix} 0 \\ 0 \\ 0 \\ 0 \\ 0 \\ 0 \\ 0 \\ 0 \\ 0 \\ 0 \\ 1 \end{bmatrix},$$

where  $\mathbf{Q}^{00}$  is the  $11 \times 11$  unit matrix,  $\mathbf{E}^{00}$  is a vector describing homogeneous deformation forms, and  $\mathbf{E}^{01}$ ,  $\mathbf{E}^{10}$ , and  $\mathbf{E}^{11}$  are vectors describing higher deformation forms. Hereinafter,  $r_1, r_2 = 0, 1$ .

For the resulting stresses, according to the method of double approximation [17], we assume a similar approximation:

$$\mathbf{H} = \sum_{r_1, r_2} \mathbf{Q}^{r_1 r_2} \mathbf{H}^{r_1 r_2} \xi_1^{r_1} \xi_2^{r_2}, \quad \mathbf{L} = \sum_{r_1, r_2} \mathbf{Q}^{r_1 r_2} \mathbf{L}^{r_1 r_2} \xi_1^{r_1} \xi_2^{r_2}. \quad (12)$$

In this case, for the vectors  $\mathbf{H}^{r_1 r_2}$  and  $\mathbf{L}^{r_1 r_2}$ , we use formulas similar to (11).

Let us introduce displacements (9), strains (10), and resulting stresses (12) into Eq. (8) and, using the standard variational procedure of the mixed model, write the FEM equations

$$\mathbf{E}^{r_1 r_2} = (\mathbf{Q}^{r_1 r_2})^T \mathbf{B}^{r_1 r_2} \mathbf{u}, \quad \mathbf{H}^{r_1 r_2} = (\mathbf{Q}^{r_1 r_2})^T \mathbf{D} \mathbf{Q}^{r_1 r_2} \mathbf{E}^{r_1 r_2}, \quad (13)$$

$$\sum_{r_1, r_2} \frac{1}{3^{r_1 + r_2}} [(\mathbf{B}^{r_1 r_2})^T \mathbf{Q}^{r_1 r_2} \mathbf{H}^{r_1 r_2} + 2(\mathbf{R}^{r_1 r_2} \mathbf{u})^T \mathbf{Q}^{r_1 r_2} \mathbf{L}^{r_1 r_2}] = \mathbf{F},$$

where  $\mathbf{u} = [\mathbf{v}_1^T \ \mathbf{v}_2^T \ \mathbf{v}_3^T \ \mathbf{v}_4^T]^T$  is the vector of nodal displacements of the element,  $\mathbf{F}$  is the vector of nodal loads,  $\mathbf{B}^{r_1 r_2}$  are  $11 \times 24$  deformation matrices corresponding to the linear components of the strain tensor,  $\mathbf{R}^{r_1 r_2}$  are three-dimensional  $11 \times 24 \times 24$  deformation arrays corresponding to the nonlinear components of the strain tensor. In this case,  $\mathbf{R}^{r_1 r_2} \mathbf{u}$  are  $11 \times 24$  matrices whose elements are calculated from the formulas

$$(\mathbf{R}^{r_1 r_2} \mathbf{u})_{pq} = \sum_s R_{pqs}^{r_1 r_2} u_s \quad (p = \overline{1, 11}; q, s = \overline{1, 24}).$$

Excluding the vectors  $\mathbf{E}^{r_1 r_2}$  and  $\mathbf{H}^{r_1 r_2}$  from Eqs. (13), we obtain the resolving matrix equation

$$(\mathbf{K} + \mathbf{K}_\tau) \mathbf{u} = \mathbf{F}, \quad (14)$$

where  $\mathbf{K}$  is the stiffness matrix of the element and  $\mathbf{K}_\tau$  is the matrix of geometrical stiffness.

It is noteworthy that, from Eqs. (13), immediately follow the relations [9]

$$\begin{aligned} hE_{33}^{10} &= A_1 \bar{\xi}_1 (E_{13}^{+00} - E_{13}^{-00}), & hE_{33}^{01} &= A_2 \bar{\xi}_2 (E_{23}^{+00} - E_{23}^{-00}), \\ hE_{33}^{11} &= A_1 \bar{\xi}_1 (E_{13}^{+01} - E_{13}^{-01}), & hE_{33}^{10} &= A_2 \bar{\xi}_2 (E_{23}^{+10} - E_{23}^{-10}), \end{aligned} \quad (15)$$

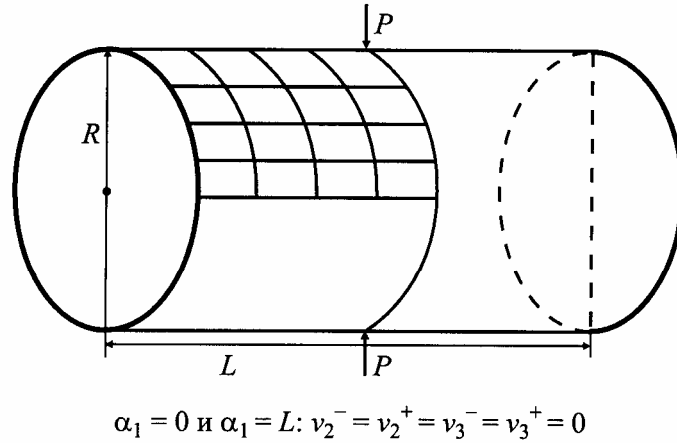


Fig. 2. Cylindrical shell under the action of two radial forces.

TABLE 1. Normalized Radial Displacement at the Force Application Point

Mesh	SRI [20]	RSDS [21]	MITC4 [22]	Mixed [23]	QPH [24]	TMS4
4 × 4	0.373	0.469	0.370	0.399	0.370	0.883
8 × 8	0.747	0.791	0.740	0.763	0.740	0.934
16 × 16	0.935	0.946	0.930	0.935	0.930	0.979

which means that only seven higher approximation forms of strains (for example,  $E_{11}^{-01}$ ,  $E_{11}^{+01}$ ,  $E_{22}^{-10}$ ,  $E_{22}^{+10}$ ,  $E_{13}^{-01}$ ,  $E_{13}^{+01}$ , and  $E_{23}^{-10}$ ) among the eleven ones introduced in Eqs. (10) and (11) are independent. Relations (15) ensure the necessary number of degrees of freedom for the element, and thus the stiffness matrix  $\mathbf{K}$  has exactly six zero eigenvalues, which is necessary for a precise representation of small displacements of the element as a rigid unit [9].

We should also note that the stiffness matrix of the element was calculated based on precise analytical integration. As a result, we succeeded in constructing a universal and very efficient element, which does not admit false displacements (mechanisms) and is not subjected to the membrane, shear [11], or Poisson locking [18]. The developed TMS4 element and its nonlinear analog (which will be considered in the second report) served as the basis for the TIRANA (Tire Analysis) software package intended for use in the tire industry.

## Numerical Results and Discussion

Let us consider the bending problem for a closed circular cylindrical shell, with rigid diaphragms on its ends, under the action of a self-balanced system of two point forces (Fig. 2). The shell has the following mechanogeometrical characteristics [19]:  $R = 300$ ,  $L = 600$ ,  $h = 3$ ,  $E = 3 \cdot 10^6$ ,  $\nu = 0.3$ , and  $P = 1$ . A feature of the problem is that the stress state is close to pure bending, which complicates the application of the FEM. Owing to symmetry, only one octant of the cylinder was considered. Table 1 presents the results of calculating the radial displacement at the point of application of the force. The displacement is normalized to a computationally precise value equal to  $-1.837 \times 10^{-5}$ , which was obtained by using rather fine meshes. Table 1 also shows the displacements obtained in [20-24] by means of bilinear isoparametric elements and normalized in [25] to the analytical solution  $-1.8245 \times 10^{-5}$  based on the classical Timoshenko-type shell theory. As is

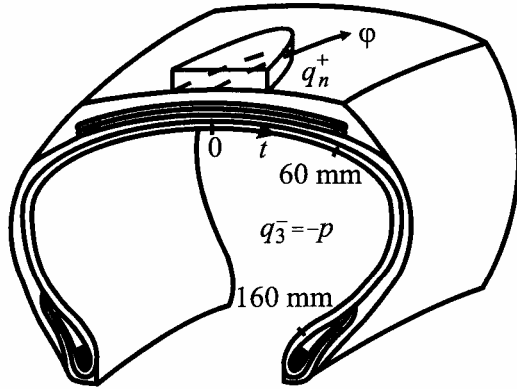


Fig. 3

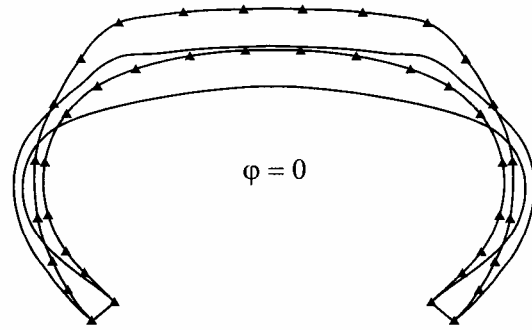


Fig. 4

Fig. 3. Calculation of a 175/70R13 radial car tire.

Fig. 4. Deformed profiles of a 175/70R13 tire subjected to internal pressure (-▲-) and to an additional local load (—).

TABLE 2. Tire Deflection at the Center of the Loading Area

Loading	I	II	III	IV	[27]
$c$	0	$q_0/3$	$2q_0/3$	$q_0$	
$d$	$q_0$	$q_0/2$	0	$-q_0/2$	
$v_3^+(0, 0)$ , mm	15.0	14.4	13.7	13.1	18.0

seen, on rough meshes, the TMS4 element demonstrates quite a good productivity, excelling in this test the isoparametric elements mentioned above, which can be explained by the use of deformational relations precisely representing the displacement of the shell as a rigid body.

As a second example, we will consider the problem of local loading of a rubber-cord shell of revolution — a 175/70R13 radial car tire (Fig. 3). First, the tire was subjected to an internal pressure of  $p = 0.2$  MPa. This axisymmetric problem was solved based on the Timoshenko-type shell theory, with regard for transverse compression, in the geometrically nonlinear statement with the help of the numerical algorithm constructed in [7]. Then, for the prestressed rubber-cord shell subjected to a load

$$q_n^+ = -c - d \sqrt{1 - \frac{t^2}{a^2} - \frac{\varphi^2}{\Delta^2}}, \quad \frac{t^2}{a^2} + \frac{\varphi^2}{\Delta^2} \leq 1, \quad (16)$$

locally distributed inside an ellipse with semiaxes  $a$  and  $\Delta$  on the outer surface perpendicularly to the rotation axis of the shell, where  $t$  and  $\varphi$  are the arc and circumferential coordinates of the inner surface of the tire, the linear problem was solved by using the bilinear TMS4 element (a geometrically nonlinear problem is considered in the second report). In all, we considered four types of local loads distributed inside an ellipse with  $a = 50$  mm and  $\Delta = \pi/10$  rad. As a result, the area of the load region turned out to be  $\Omega = 13,520$  mm<sup>2</sup>, which corresponded to experimental data. The values of the coefficients  $c$  and  $d$  in Eq. (16), in the case of loading the tire by a resulting compression force of  $P = 3$  kN, which were calculated from the formula  $P = (c + 2d/3)\Omega$  ( $q_0 = 0.333$  MPa), are given in Table 2. In these calculations, it was assumed that the ends of the tire at  $t = \pm 160$  mm were rigidly fixed. This situation, on the whole, is rather realistic and is considered in [26].



Figure 4 shows the deformed profile of the tire at  $\varphi = 0$  for loading type III. For the remaining loading cases, the deformed profiles practically were the same, therefore they are not shown in Fig. 4. For comparison, Table 2 gives the maximum deflection of the outer contour of the tire for all the loads considered and the experimental data from [27]. As is seen, the calculation results, especially for loading type I, are quite satisfactory considering the fact that the problem of local loading of the tire was solved in the linear statement. In a geometrically nonlinear statement, the deformed profiles of the tire, for all loading types modeling the contact pressure, differ considerably. In this case, the best agreement between calculation and experimental data is reached for loading type III.

## REFERENCES

1. M. Kulikov, "Nonaxisymmetric loading of a prestressed multilayered reinforced shell," *Mech. Compos. Mater.*, **26**, No. 2, 254-258 (1990).
2. E. I. Grigolyuk and G. M. Kulikov, "Local loading of rubber-cord shells of revolution," *Mech. Compos. Mater.*, **27**, No. 4, 436-441 (1991).
3. G. M. Kulikov, "Computational models for multilayered composite shells with application to tires," *Tire Sci. Techn.*, **24**, No. 1, 11-38 (1996).
4. G. M. Kulikov, F. Bohm, A. Duda, and R. Wille, "Zur inneren Mechanik des Radialreifens. Teil 1.: Geschichtete Kompositschale mit globalem Verschiebungsansatz für das Gesamtlaminat," *Techn. Mech.*, **20**, 1-12 (2000).
5. A. K. Noor and J. A. Tanner, "Advances and trends in the development of computational models for tires," *Comput. Struct.*, **20**, 517-533 (1985).
6. A. K. Noor and W. S. Burton, "Assessment of computational models for multilayered composite shells," *Appl. Mech. Rev.*, **43**, 67-97 (1990).
7. G. M. Kulikov and S. V. Plotnikova, "Comparative analysis of two algorithms for numerical solution of nonlinear static problems for multilayered anisotropic shells of revolution. 2. Account of transverse compression," *Mech. Compos. Mater.*, **35**, No. 4, 293-300 (1999).
8. G. M. Kulikov and S. V. Plotnikova, "Numerical solution of a contact problem for multilayer composite plates," *Vestn. Tamb. Gos. Tekhn. Univer.*, **4**, 526-539 (1998).
9. G. M. Kulikov and S. V. Plotnikova, "Simple and effective elements based upon Timoshenko–Mindlin shell theory," *Comput. Meth. Appl. Mech. Eng.*, **191**, 1173-1187 (2002).
10. G. M. Kulikov and S. V. Plotnikova, "Finite-element formulation of straight composite beams undergoing finite rotations," *Trans. TSTU*, **7**, 617-633 (2001).
11. A. I. Golovanov and N. S. Kornishin, *Introduction to the Finite-Element Method for the Statics of Thin Shells* [in Russian], KFTI AN SSSR, Kazan' (1989).
12. R. B. Rikards, *Finite-Element Method in the Theory of Shells and Plates* [in Russian], Zinatne, Riga (1988).
13. G. M. Kulikov, "Refined global approximation theory of multilayered plates and shells," *J. Eng. Mech.*, **127**, 119-125 (2001).
14. K. Washizu, *Variational Methods in Elasticity and Plasticity*, Pergamon Press, Oxford (1975).
15. A. S. Sakharov and I. Altenbach (eds.), *Finite-Element Method in Mechanics of Solid Bodies* [in Russian], Vishcha Shkola, Kiev (1982).
16. T. J. R. Hughes and T. E. Tezduyar, "Finite elements based upon Mindlin plate theory with particular reference to the four-node bilinear isoparametric element," *Trans. ASME, J. Appl. Mech.*, **48**, 587-596 (1981).
17. G. Wempner, D. Talaslidis, and C. M. Hwang, "A simple and efficient approximation of shells via finite quadrilateral elements," *Trans. ASME, J. Appl. Mech.*, **49**, 115-120 (1982).
18. M. Bischoff and E. Ramm, "On the physical significance of higher order kinematic and static variables in a three-dimensional shell formulation," *Int. J. Solids Struct.*, **37**, 6933-6960 (2000).

19. G. R. Heppler and J. S. Hansen, "A Mindlin element for thick and deep shells," *Comput. Meth. Appl. Mech. Eng.*, **54**, 21-47 (1986).
20. T. J. R. Hughes and W. K. Liu, "Nonlinear finite element analysis of shells. Part II. Two-dimensional shells," *Comput. Meth. Appl. Mech. Eng.*, **27**, 167-182 (1981).
21. D. Lam, W. K. Liu, E. S. Law, and T. Belytschko, "Resultant-stress degenerated-shell element," *Comput. Meth. Appl. Mech. Eng.*, **55**, 259-300 (1986).
22. K. J. Bathe and E. N. Dvorkin, "A formulation of general shell elements — the use of mixed interpolation of tensorial components," *Int. J. Numer. Meth. Eng.*, **22**, 697-722 (1986).
23. J. C. Simo, D. D. Fox, and M. S. Rifai, "On a stress resultant geometrically exact shell model. Part II. The linear theory; computational aspects," *Comput. Meth. Appl. Mech. Eng.*, **73**, 53-92 (1989).
24. T. Belytschko and I. Leviathan, "Physical stabilization of the 4-node shell element with one-point quadrature," *Comput. Meth. Appl. Mech. Eng.*, **113**, 321-350 (1994).
25. J. H. Argyris, M. Papadrakakis, C. Apostolopoulou, and S. Koutsourelakis, "The TRIC shell element: theoretical and numerical investigation," *Comput. Meth. Appl. Mech. Eng.*, **182**, 217-245 (2000).
26. E. I. Grigolyuk and G. M. Kulikov, *Multilayer Reinforced Shells. Calculation of Pneumatic Tires* [in Russian], Mashinostroenie, Moscow (1988).
27. A. E. Belkin, B. L. Bukhin, O. N. Mukhin, and N. L. Narskaya, "Some models and methods of pneumatic tire mechanics," in: F. Böhm and H. P. Willumeit (eds.), *Tyre Models for Vehicle Dynamic Analysis* (1997), pp. 250-271.